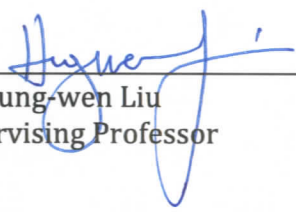


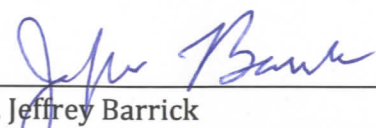
# *In vitro* reconstitution of TDP-2-deoxynogalamine

*Presented by Tianlu Ma*

*In partial fulfillment of the requirements for graduation with the Dean's Scholars Honors Degree in Biochemistry*

  
\_\_\_\_\_  
Dr. Hung-wen Liu  
Supervising Professor

4/24/2014  
Date

  
\_\_\_\_\_  
Dr. Jeffrey Barrick  
Honors Advisor in Biochemistry

4/16/2014  
Date

## ABSTRACT

Nogalamycin is an anthracycline compound produced by *Streptomyces nogalater*. Anthracyclines have been shown to be highly effective against cancer tissues, and anthracyclines such as daunorubicin are at the center of many chemotherapy treatments. However, anthracyclines are also highly toxic, particularly to the heart, making it necessary for the continuing study of this group of compounds. Similar to other anthracyclines, nogalamycin also shows antitumor activity. However, also similar to many other anthracyclines, its cardiotoxicity precludes its use as a clinical drug. In the past, semisynthesis has been successful in producing anthracycline analogs that have greater efficacy and lower cardiotoxicity. However, the success rate has been very low, with only a handful of potential candidates out of thousands of new compounds ever making it to clinical trials. Therefore, a more efficient way of generating new anthracyclines is needed to find better chemotherapy drugs. Towards this end, we have expressed and purified several proteins in the nogalamycin biosynthesis gene cluster in order to better understand how nature produces these products and harness that knowledge for future bioengineering efforts. Specifically, we have focused on the enzymes involved in modification and synthesis of nogalamine, the amino sugar essential for nogalamycin activity, and assayed the activities of SnogF, SnogG, SnogA, and SnogX.

## INTRODUCTION

### **Anthracyclines**

Anthracyclines are aromatic polyketides produced by many Streptomycetes. These compounds contain an aglycone chromophore with one or more deoxysugars, usually including an amino sugar typically attached at C-7 on ring A (Minotti & Menna et al., 2004). The first anthracyclines, doxorubicin (**Figure 1a**) and daunorubicin (**Figure 1b**), were purified in the 1960s from *Streptomyces peucetius* (Weiss, 1992). Since their discovery, anthracyclines have proven to be among the most effective chemotherapy drugs available today. The drugs work by a variety of mechanisms including generation of reactive oxygen species and inhibition of topoisomerases (Gewirtz, 1999). Notably, the planar shape of anthracyclines allows for intercalation into DNA, with the charged amino sugars interacting with the minor groove of the double helix, resulting in interference in DNA-dependent RNA synthesis, (Nunn & Van Meervelt et al., 1991). However, while effective, these compounds are also highly toxic, particularly to heart tissue (Minotti & Menna et al., 2004). For this reason, anthracyclines have continued to be compounds of great interest. In particular, great efforts have been made to find and synthesize new anthracyclines with improved efficacy and lower cardiotoxicity. These efforts have been partly successful, and anthracyclines such as epirubicin (**Figure 1c**) and idarubicin (**Figure 1d**), semisynthetic derivatives of doxorubicin and daunorubicin, respectively, are in common use today as antitumor drugs (Minotti & Menna et al., 2004).

The process of finding epirubicin and idarucin has led to the development of a large variety of new compounds, including over 2000 analogs of the original

anthracyclines daunorubicin and doxorubicin (Weiss, 1992). This is due to the great variability in the anthracycline structure, and even a modest change in the compound can lead to drastic differences in biological activity. For example, the aglycone core of anthracyclines can be modified in a variety of ways. Idarubicin is identical to daunorubicin with the exception of the lack of a methoxy group at C-4 on ring D (Minotti & Menna et al., 2004). This one change gives idarubicin activity against a greater variety of cancers and allows for oral administration of the drug (Borchmann & Hubel et al., 1997; Toffoli & Sorio et al., 2000). *In vitro* studies have also suggested that idarubicin is more effective than daunorubicin against cell lines that have developed multidrug resistance (Toffoli & Simone et al., 1994). Additionally, the sugar bound to C-7 of ring A can be modified in many ways. In epirubicin, which is otherwise identical to doxorubicin, the hydroxyl group at C-4' of daunosamine is in an equatorial rather than an axial position (Minotti & Menna et al., 2004). This variation introduces pharmacokinetic and metabolic changes that lead to a cumulative dose limit of epirubicin that is twice that of doxorubicin (Robert, 1993). However, despite these improvements, these drugs still carry a significant risk for cardiotoxicity. In addition, with only a handful out of the 2000 analogs ever making it to clinical trials, it becomes apparent that more efficient ways of producing novel anthracyclines are needed. It continues to be important to characterize and understand the natural synthesis of anthracyclines in order to harness nature's pathways for the production of more effective and less toxic drugs.

### **Nogalamycin**

Nogalamycin (**Figure 2a**) is an anthracycline discovered in 1965 from *Streptomyces nogalater* (Bhuyan & Smith, 1965). Unlike the other anthracyclines

previously discussed, nogalamycin has two sugars. One is nogalose, a neutral deoxysugar as opposed to the usual amino sugar, attached at the C-7 position on ring A. The second is an amino sugar found on ring D, bound at both C-1 via an *O*-glycosidic bond and a rare carbon-carbon bond at C-2 (Wiley, 1979). This latter unusual glycosyl bond effectively introduces two additional rings to the aglycone core. Additionally, this second sugar allows nogalamycin to interact with both the minor and major grooves of DNA, making the compound highly active against Gram-positive bacteria and several cancer cell lines (Liaw & Gao et al., 1989; Williams & Egli et al., 1990; Smith & Davies et al., 1995). Unfortunately, nogalamycin is also highly cytotoxic, never even making it to clinical trials (Li & Krueger, 1991). Due to its high activity, however, nogalamycin continued to be an attractive research candidate, and menogaril (**Figure 2b**) was semisynthetically derived from nogalamycin in the 1970s by the removal of the uncharged nogalose on C-7 and a methyl ester group from C-10. While these changes led to greater anticancer activity and lower toxicity than doxorubicin, clinical trials of menogaril were halted at Phase II (Li & Krueger, 1991; Siitonen & Claesson et al., 2012).

Much of the current effort is focused on semisynthesis and degradation to find new anthracyclines and modify existing anthracyclines, seeking novel compounds that are more effective and safer (Wiley, 1979; Li & Krueger, 1991). However, studying and understanding how anthracycline molecules are naturally produced can greatly help accomplish both goals. The gene cluster for biosynthesis of nogalamycin was identified and sequenced in the 1990s (Ylihonko & Tuikkanen et al., 1996; Torkkell & Kunnari et al., 2001). Since then, many of the proteins encoded have been identified and assayed (Torkkell & Kunnari et al., 2001). However, many of the late-stage glycosylation steps,

particularly the synthesis and modification of the sugars, are still unclear. Our work here was performed with the purpose of elucidating some of these steps. Ultimately, we aim to find the mechanism by which the carbon-carbon bond between C2 of the aglycone and C5 of the nogalamine is formed. To do this, we must first characterize how the amino sugar is made by *S. nogalater*. To this end, we have identified the proteins and steps involved in the biosynthesis of TDP-2-deoxynogalamine.

### **Nogalamine**

**Figure 3** shows the structure of TDP-activated 2-deoxynogalamine. Bacterial sugars usually follow highly conserved biosynthesis pathways, beginning with TDP-activated intermediates (Thibodeaux & Melancon et al., 2008). The nogalamycin gene cluster encodes proteins that show homology with conserved proteins in other bacteria, and hint that nogalamine follows a pathway similar to other bacterial sugars (Torkkell & Kunnari et al., 2001; Siitonen & Claesson et al., 2012). Specifically, while nogalamine as bound to nogalamycin contains a 2' hydroxyl group, the presence of a 2',3'-dehydratase (SnogH) and the absence of a 3',4'-ketoisomerase suggest that the 2' hydroxyl is first removed then reinstalled afterwards, perhaps after the attachment of nogalamine to the aglycone core (Siitonen & Claesson et al., 2012). Therefore, the enzymes encoded by *snogJ*, a thymidylyl transferase, *snogK*, a 4',6'-dehydratase, and *snogH*, a 2',3'-dehydratase, most likely catalyze the first three steps in nogalamine biosynthesis (Torkkell & Kunnari et al., 2001; Siitonen & Claesson et al., 2012).

Following these three steps, there is some ambiguity in the pathway. The stereochemistry of the product of the 3'-aminotransferase SnogI is unknown. However, based on similarity to other deoxy amino sugar pathways and the structure of

nogalamycin, we predict that SnogI will introduce an equatorial amino group (Hong & Zhao et al., 2008). Additionally, the gene cluster for nogalamycin encodes only one sugar epimerase, SnogF. Given that both nogalamine and nogalose are likely formed through L-configured intermediates, it is necessary that both pathways must share this enzyme (Torkkell & Kunnari et al., 2001; Siitonen & Claesson et al., 2012). Nogalamine further requires a 4'-ketoreductase, and there are two such enzymes, SnogG and SnogC, encoded in the gene cluster (Torkkell & Kunnari et al., 2001, Metsa-Ketela & Niemi et al., 2008). It is unknown which enzyme is actually involved in nogalamine biosynthesis. Based on phylogenetic comparison with other deoxy amino sugar 4'-ketoreductases, we predict that SnogG is the enzyme involved in the synthesis of nogalamine. Finally, the nogalamycin gene cluster encodes two *N*-methyltransferases, SnogA and SnogX (Torkkell & Kunnari et al., 2001). It is unknown which methyltransferase is needed for the methylation of nogalamine or which order the enzymes work in if both are needed. Therefore, we have expressed and purified the proteins involved for *in vitro* reconstitution of TDP-2-deoxynogalamine and performed assays to analyze the roles of SnogF, SnogG, SnogA, and SnogX in the biosynthesis of this sugar.

## MATERIALS AND METHODS

### **Protein Expression and Purification**

RfbB, TylX3, and EvaB were purified as previously reported in the literature (Takahashi & Liu et al., 2005 and 2006).

Genomic DNA was isolated and purified from *Streptomyces nogalater* NRRL 3035 using the Qiagen DNeasy Blood and Tissue kit. From this, *snogF*, *snogG*, *snogA*,

and *snogX* were cloned with 5'-*ndel* and 3'-*nheI* restriction sites. The products were verified by sequencing at the UT DNA sequencing facility. Correct products were digested using NdeI/NheI then ligated into pET28b for expression with N-terminal His<sub>6</sub>-tags. The resulting plasmids were used to transform BL21 (DE3), and positive clones were selected with 30 µg/mL kanamycin. The *snogA* and *snogF* cultures were induced at OD600 ≈ 0.6 with 100 µM IPTG and grown for 16 hr at 16 °C. The *snogX* culture was induced at OD600 ≈ 0.6 with 200 µM IPTG and grown for 16 hr at 30 °C. The *snogG* culture was induced at OD600 ≈ 0.6 with 200 µM IPTG and grown for 16 hr at 25 °C. Cultures were collected by centrifugation at 4500 x g at 4 °C. The cell pellets were then stored at -80 °C until lysis.

The cell pellets were thawed in room temperature water and resuspended in two volumes of lysis buffer (**Table 1**). After adding 1 mg/mL of lysozyme, cell suspensions were incubated on ice for 30 min. The suspensions were sonicated in 30-sec bursts with a one-min rest between each burst. The resulting suspensions were centrifuged at 20000 x g at 4 °C for 40 min. The supernatants were added to 6.5 mL of pre-packed, equilibrated Ni-NTA resin. The columns were washed with approximately 100 mL of wash buffer (**Table 1**) and then eluted using elution buffer (**Table 1**). Samples from each fraction were analyzed by SDS-PAGE, and fractions containing a significant amount of protein were pooled and dialyzed. The eluates were then concentrated to 5-8 mL using an Amicon stirred cell under N<sub>2</sub>. The concentrated proteins were frozen in liquid nitrogen and stored at -80 °C until assays were performed. **Table 1** shows composition of all buffers used during the purification process. Buffer group A was used for SnogA, SnogF, and SnogX, and buffer group B was used for SnogG. All buffers were adjusted to pH 8.0.



## Assays and HPLC

Step 1 for all assays was incubation of TDP-glucose with RfbB at 37 °C for approximately 45 min. The enzymes, as indicated in **Table 2**, were then incubated with the previous reaction at 30 °C for 30 min to one hour. In addition to the assays listed in **Table 2**, one additional assay was performed with RfbB, SnogF, and SnogG, and a second assay was performed with RfbB, SnogF, and TylC2 to investigate the substrate flexibility of SnogG. The reactions analyzed by HPLC on a Beckman System Gold apparatus equipped with a 125 Solvent Module and 166 UV Detector Module. A Dionex Carbopac PA1 4X150 mm analytical column fitted with a Dionex Carbopac PA1 4X50 mm guard column was used. The column was run with a binary mobile phase composed of Solvent A (water) and Solvent B (500 mM ammonium acetate in water), and compounds were detected at 267 nm. **Figure 4** shows the gradients, given as percent solvent B over time in minutes, used for HPLC, where **4a** shows the gradient first used and **4b** shows the gradient used to separate monomethylated and dimethylated TDP-2-deoxynogalamine. Peaks were collected, and ESI-MS and one- and two-dimensional (COSY) <sup>1</sup>H-NMR were used to identify products.

## RESULTS

**Figures 5-8** shows the HPLC traces for the assays listed in **Table 2**. As seen in **Figure 5**, incubation of the full set of enzymes (RfbB, TylX3, EvaB, SnogF, SnogG, SnogA, and SnogX) leads to the production of three compounds. The top trace in **Figure 5** shows two peaks, the earlier peak containing both **7** and **8**, mono- and dimethylated nogalamine, respectively, while the later peak contains the intermediate **6**. Using gradient

**4b**, the first peak was resolved into two separate peaks for **7** and **8**, as seen in the bottom trace of **Figure 5**. Mass spectrometry data support these peak assignments, and <sup>1</sup>H-NMR for **6** agree with previously published results.

**Figure 6** shows HPLC traces for assays concerning the roles of SnogF and SnogG in the production of TDP-2-deoxynogalamine. In assay 2, the absence of SnogA and SnogX produced only one peak corresponding to **6**, but no peaks were detected for **7** and **8**. The peak for **6** also disappears without the presence of both SnogF and SnogG. In assay 3, without either SnogF or SnogG, a peak corresponding to **4** can be seen. When only SnogF was present, as in assay 4, a single peak corresponding to **4** and **5** was detected. When only SnogG was present, as in assay 5, compound **5** is no longer produced, and the peak corresponds only to **4**. In all four assays, the peak corresponding to **2** could be seen later in the trace. Interestingly, when both SnogF and SnogG were present, a peak corresponding to **2b** could also be seen. To further investigate this shunt pathway, the TDP-glucose/RfbB reaction was incubated with SnogF and SnogG or SnogF and TylC2, a different 4'-ketoreductase. As can be seen in **Figure 7b**, **2b** was detected in the reaction with SnogG but not in the reaction with TylC2. Mass spectrometry data for **2b** support these peak assignments, and <sup>1</sup>H-NMR for **2b** agree with previously published results for TDP-L-rhamnose.

**Figure 8** shows HPLC traces for assays concerning the role of SnogA and SnogX in the methylation of nogalamine. When only SnogX was present as in assay 6, only **6** was produced, with very little methylated sugar detected. When only SnogA was present as in assay 7, both **6** and **7**, the monomethylated sugar, were detected. As shown in assay 1, the presence of both SnogA and SnogX leads to the production of **6**, **7**, and **8**. To

further test the sequence of SnogA and SnogX, in assay 8, SnogX was added after an initial one-hour incubation with SnogA, and this led also to the production of **6**, **7**, and **8**.

## CONCLUSION

**Figure 9a** shows the pathway for synthesis of TDP-2-deoxynogalamine based on our results. Specifically, from assays 1-5, we saw that SnogF alone produced **5**, and SnogF and SnogG together produced **6**. Additionally, we saw that SnogF and SnogG produced shunt products corresponding to rhamnose and nogalose biosynthesis, indicating that SnogF and SnogG are both substrate-flexible, suggesting that these enzymes are shared in the biosynthesis of both nogalamine and nogalose. We also saw SnogA alone was capable of producing the monomethylated sugar, but not the dimethylated sugar. However, SnogX by itself was not capable of accepting **6**, the non-methylated intermediate. However, SnogA followed by SnogX was capable of producing the final product, the dimethylated sugar. Thus, we have shown that both SnogA and SnogX are required for the dimethylation of nogalamine. Additionally, we have demonstrated that SnogA is responsible for the first methylation, followed by SnogX, and both methyltransferases can accept the TDP-deoxy sugar independent of the aglycone core. These results provide the necessary groundwork for future investigation into the unusual carbon-carbon bond found between nogalamine and the aglycone core of nogalamycin.

## REFERENCES

- Bhuyan, B. & Smith, C. (1965). Differential interaction of nogalamycin with DNA of varying base composition. *Proceedings Of The National Academy Of Sciences Of The United States Of America*, 54 (2), p. 566.
- Borchmann, P., Hubel, K., Schnell, R. & Engert, A. (1997). Idarubicin: a brief overview on pharmacology and clinical use. *International Journal Of Clinical Pharmacology And Therapeutics*, 35 (2), pp. 80--83.
- Gewirtz, D. (1999). A critical evaluation of the mechanisms of action proposed for the antitumor effects of the anthracycline antibiotics adriamycin and daunorubicin. *Biochemical Pharmacology*, 57 (7), pp. 727--741.
- Hong, L., Zhao, Z., Melancon, C. E., Zhang, H. & Liu, H. (2008). In vitro characterization of the enzymes involved in tdp-d-forsamine biosynthesis in the spinosyn pathway of *saccharopolyspora spinosa*. *Journal Of The American Chemical Society*, 130 (14), pp. 4954--4967.
- Li, L. H. & Krueger, W. C. (1991). The biochemical pharmacology of nogalamycin and its derivatives. *Pharmacology & Therapeutics*, 51 (2), pp. 239--255.
- Liaw, Y. C., Gao, Y. G., Robinson, H., Van Der Marel, G. A., Van Boom, J. H. & Wang, A. H. (1989). Antitumor drug nogalamycin binds DNA in both grooves simultaneously: molecular structure of nogalamycin-DNA complex. *Biochemistry*, 28 (26), pp. 9913--9918.

- Metsa-Ketela, M., Niemi, J., Mantsala, P. & Schneider, G. (2008). Anthracycline biosynthesis: genes, enzymes and mechanisms. *Springer*, pp. 101--140.
- Minotti, G., Menna, P., Salvatorelli, E., Cairo, G. & Gianni, L. (2004). Anthracyclines: molecular advances and pharmacologic developments in antitumor activity and cardiotoxicity. *Pharmacological Reviews*, 56 (2), pp. 185--229.
- Nunn, C. M., Van Meervelt, L., Zhang, S., Moore, M. H. & Kennard, O. (1991). DNA-drug interactions: the crystal structures of d (TGTACA) and d (TGATCA) complexed with daunomycin. *Journal Of Molecular Biology*, 222 (2), pp. 167--177.
- Robert, J. (1993). Epirubicin. clinical pharmacology and dose-effect relationship. *Drugs*, 45 (Suppl 2), pp. 20-30.
- Siitonen, V., Claesson, M., Patrikainen, P., Aromaa, M., Mantsala, P., Schneider, G. & Metsa-Ketela, M. (2012). Identification of late-stage glycosylation steps in the biosynthetic pathway of the anthracycline nogalamycin. *Chembiochem*, 13 (1), pp. 120--128.
- Smith, C. K., Davies, G. J., Dodson, E. J. & Moore, M. H. (1995). Dna-nogalamycin interactions: the crystal structure of d (TGATCA) complexed with nogalamycin. *Biochemistry*, 34 (2), pp. 415--425.
- Takahashi, H., Liu, Y., Chen, H. & Liu, H. (2005). Biosynthesis of TDP-L-mycarose: the specificity of a single enzyme governs the outcome of the pathway. *Journal Of The American Chemical Society*, 127 (26), pp. 9340--9341.

- Takahashi, H., Liu, Y. & Liu, H. (2006). A two-stage one-pot enzymatic synthesis of TDP-L-mycarose from thymidine and glucose-1-phosphate. *Journal Of The American Chemical Society*, 128 (5), pp. 1432--1433.
- Thibodeaux, C. J., Melancon, C. E. & Liu, H. (2008). Natural-product sugar biosynthesis and enzymatic glycodiversification. *Angewandte Chemie International Edition*, 47 (51), pp. 9814--9859.
- Toffoli, G., Simone, F., Gigante, M. & Boiocchi, M. (1994). Comparison of mechanisms responsible for resistance to idarubicin and daunorubicin in multidrug resistant lovo cell lines. *Biochemical Pharmacology*, 48 (10), pp. 1871--1881.
- Toffoli, G., Sorio, R., Aita, P., Crivellari, D., Corona, G., Bearz, A., Robieux, I., Colussi, A. M., Stocco, F. & Boiocchi, M. (2000). Dose-finding and pharmacologic study of chronic oral idarubicin therapy in metastatic breast cancer patients. *Clinical Cancer Research*, 6 (6), pp. 2279--2287.
- Torkkell, S., Kunnari, T., Palmu, K., Mantsala, P., Hakala, J. & Ylihonko, K. (2001). The entire nogalamycin biosynthetic gene cluster of streptomyces nogalater: characterization of a 20-kb DNA region and generation of hybrid structures. *Molecular Genetics And Genomics*, 266 (2), pp. 276--288.
- Weiss, R. B. (1992). The anthracyclines: will we ever find a better doxorubicin?. 19 (6), pp. 670--686.
- Wiley, P. F. (1979). Improved antitumor activity by modification of nogalamycin. *Journal Of Natural Products*, 42 (6), pp. 569--582.

Williams, L. D., Egli, M., Qi, G., Bash, P., Van Der Marel, G. A., Van Boom, J. H., Rich, A. & Frederick, C. A. (1990). Structure of nogalamycin bound to a DNA hexamer.

*Proceedings Of The National Academy Of Sciences*, 87 (6), pp. 2225--2229.

Ylihonko, K., Tuikkanen, J., Jussila, S., Cong, L. & Mantsala, P. (1996). A gene cluster involved in nogalamycin biosynthesis from streptomyces nogalater: sequence analysis and complementation of early-block mutations in the anthracycline pathway. *Molecular And General Genetics MGG*, 251 (2), pp. 113--120.

## APPENDIX A: TABLES

**Table 1: Buffers used for protein purification.**

		Lysis Buffer	Wash Buffer	Elution Buffer
Group A (SnogA, SnogF, SnogX)	NaH <sub>2</sub> PO <sub>4</sub>	50 mM	50 mM	50 mM
	NaCl	300 mM	300 mM	300 mM
	Imidazole	10 mM	20 mM	250 mM
	Glycerol	20%	20%	20%
Group B (SnogG)	NaH <sub>2</sub> PO <sub>4</sub>	50 mM	50 mM	50 mM
	NaCl	300 mM	300 mM	300 mM
	Imidazole	10 mM	20 mM	250 mM
	Glycerol	20%	20%	20%
	L-arginine	10 mM	10 mM	10 mM
	L-glutamate	10 mM	10 mM	10 mM
	DTT	0.5 mM	0.5 mM	0.5 mM

**Table 2: *in vitro* assays performed. ✓ indicate the protein was added to the reaction. ✗ indicates the protein was not added to the reaction. ✗/✓ indicates the protein was added after the reaction had already started. That is, for assay 8, all proteins except for SnogX was first added, and this reaction was incubated for one hour before SnogX was added.**

Assay	1	2	3	4	5	6	7	8	9
RfbB	✓	✓	✓	✓	✓	✓	✓	✓	✓
TylX3	✓	✓	✓	✓	✓	✓	✓	✓	✗
EvaB	✓	✓	✓	✓	✓	✓	✓	✓	✗
SnogF	✓	✓	✗	✓	✗	✓	✓	✓	✓
SnogG	✓	✓	✗	✗	✓	✓	✓	✓	✓
SnogA	✓	✗	✗	✗	✗	✗	✓	✓	✗
SnogX	✓	✗	✗	✗	✗	✓	✗	✗/✓	✗



APPENDIX B: FIGURES

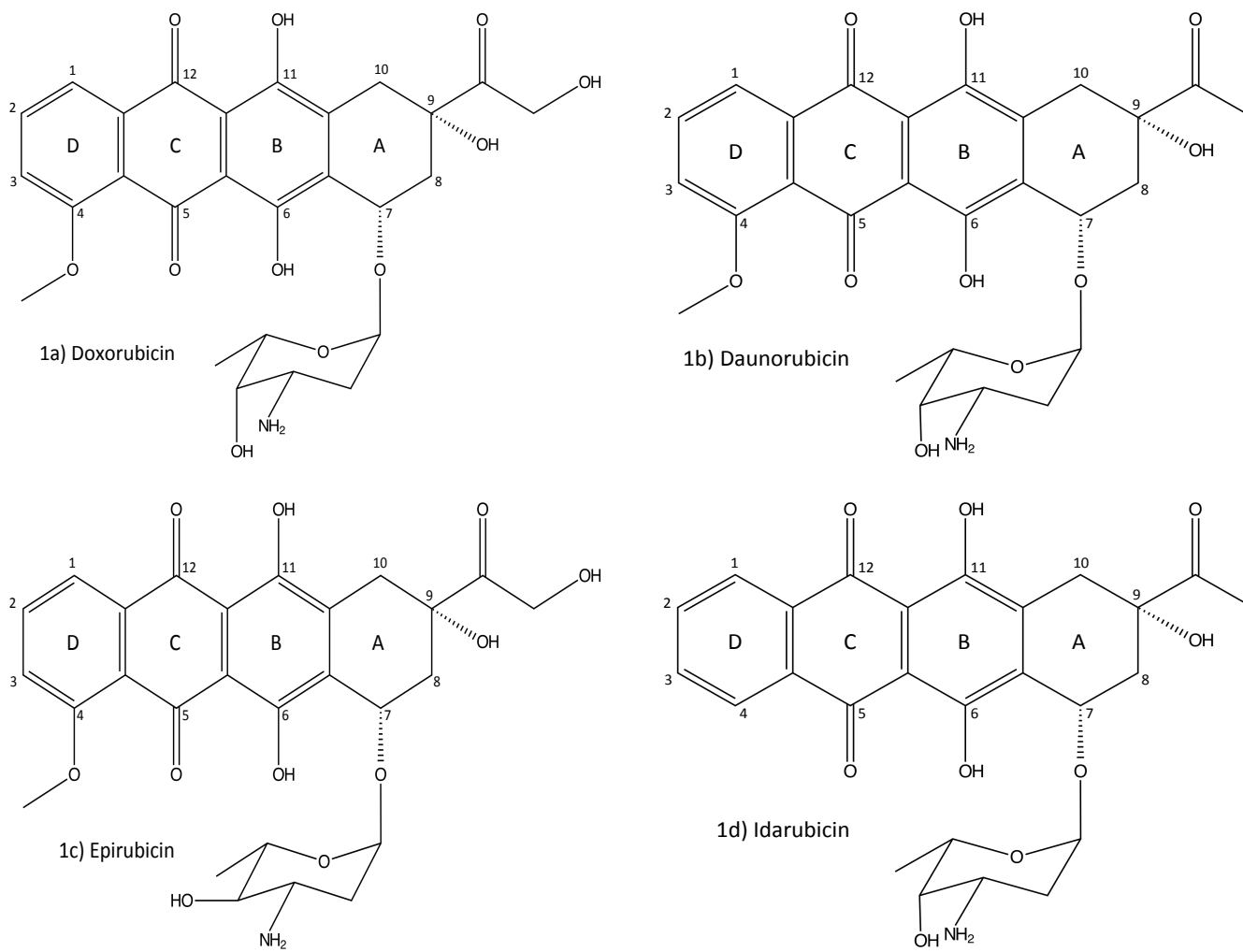


**Figure 1: Structures of a) doxorubicin, b) daunorubicin, c) epirubicin, and d) idarubicin.**

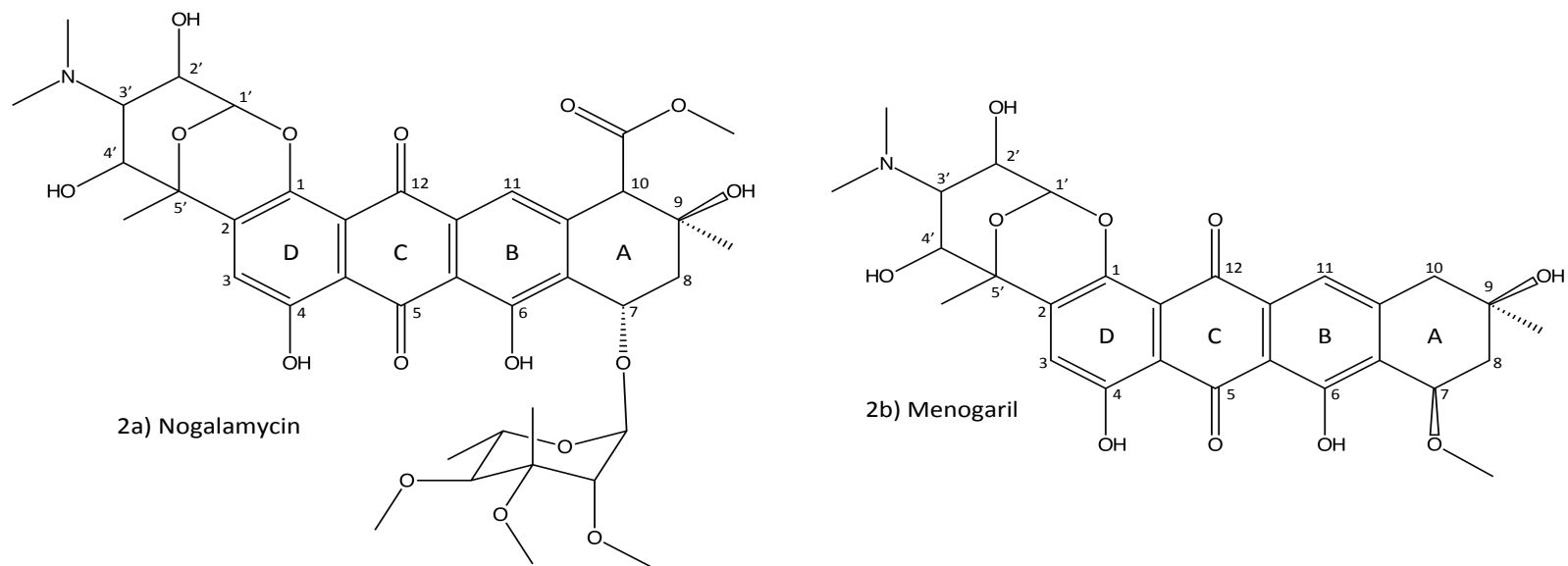


Figure 2: Structures of a) nogalamycin and b) menogaril.

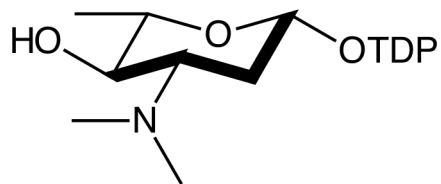
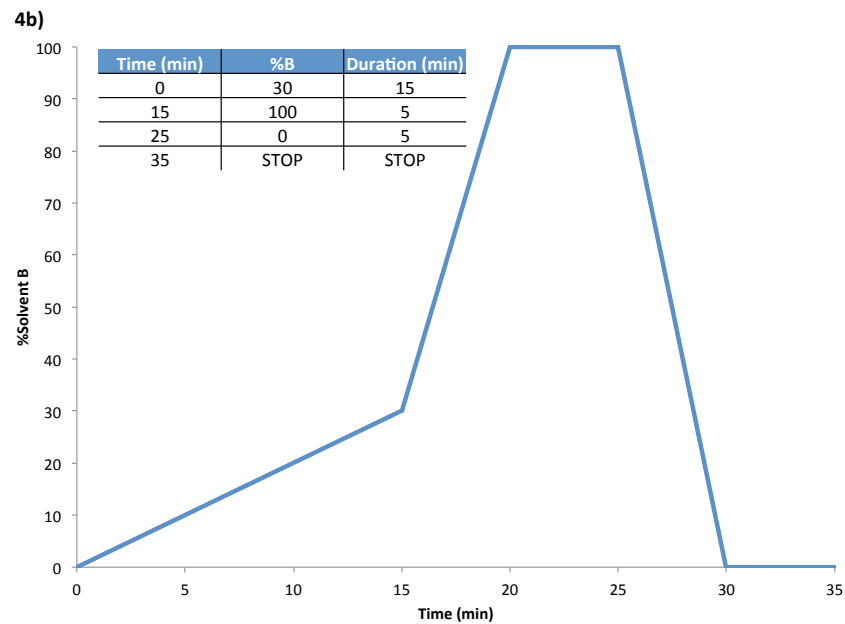
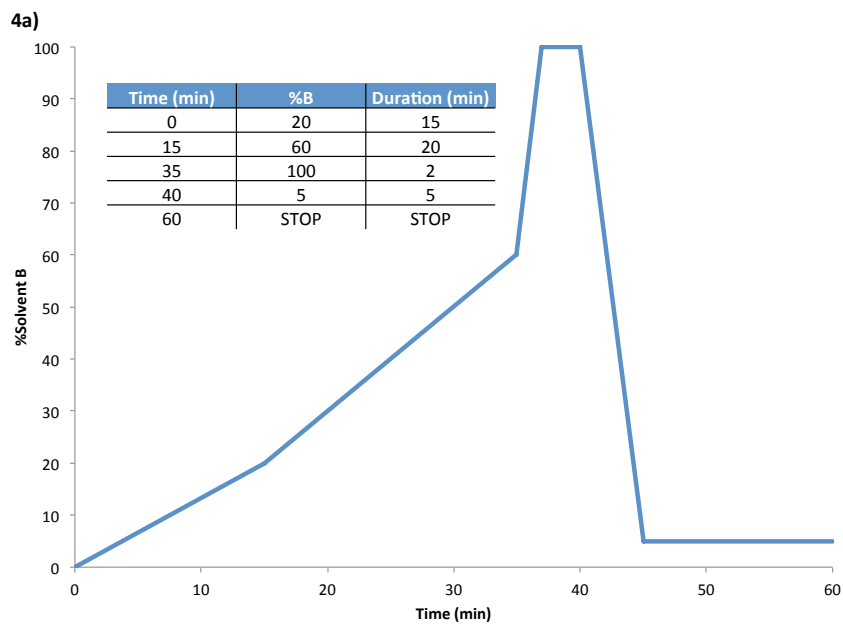


Figure 3: Structure of TDP-2-deoxynogalamine.



**Figure 4: HPLC gradients used for assay analysis shown as %B in the binary mobile phase. a) Initial gradient used for compound detection. b) Modified gradient for separation of mono- and dimethylated amino sugar.**

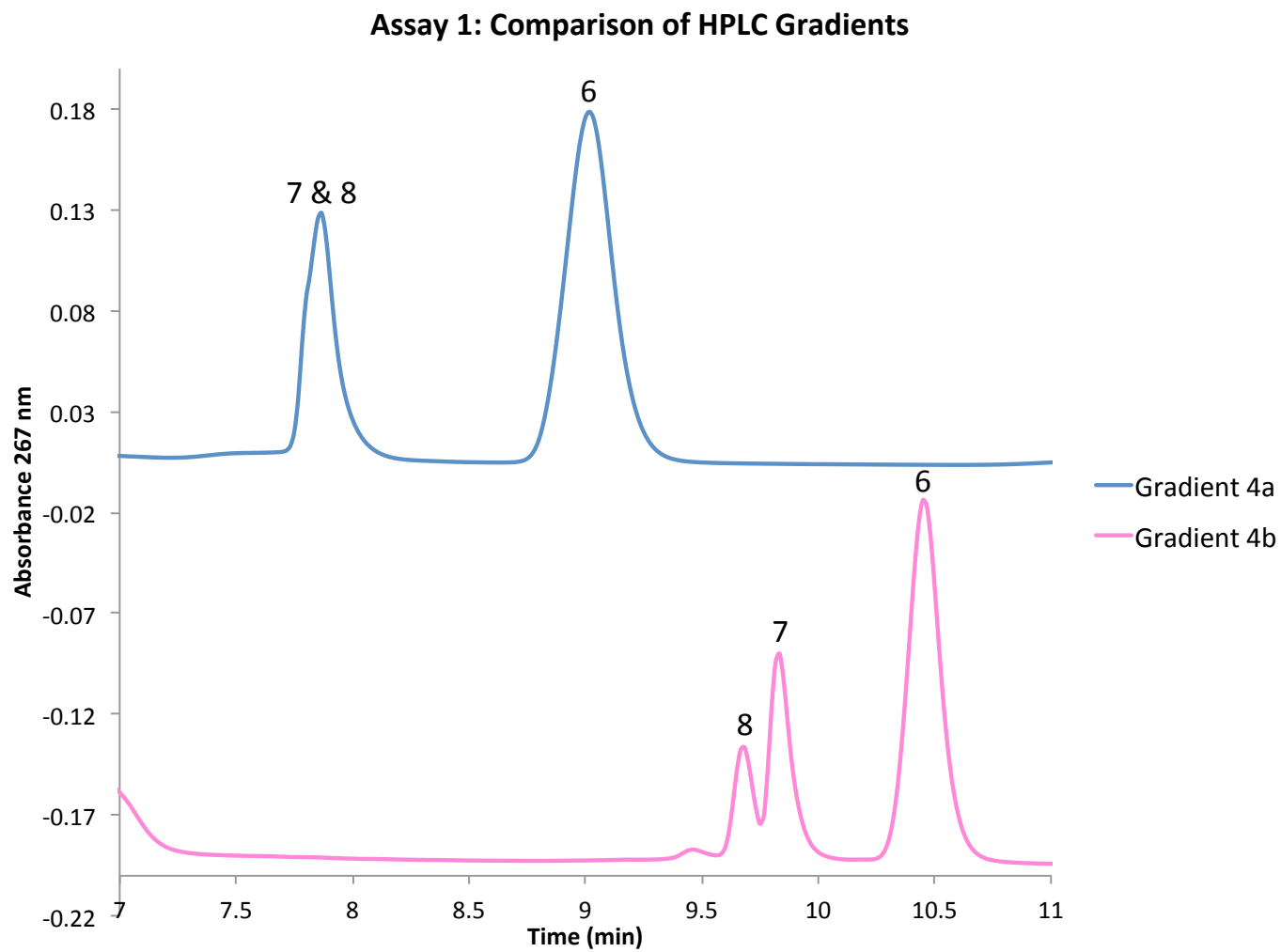


Figure 5: HPLC trace for Assay 1. The top trace results from gradient 4a, and the bottom trace results from gradient 4b, which separated the mono- and dimethylated sugars, 7 and 8, respectively.

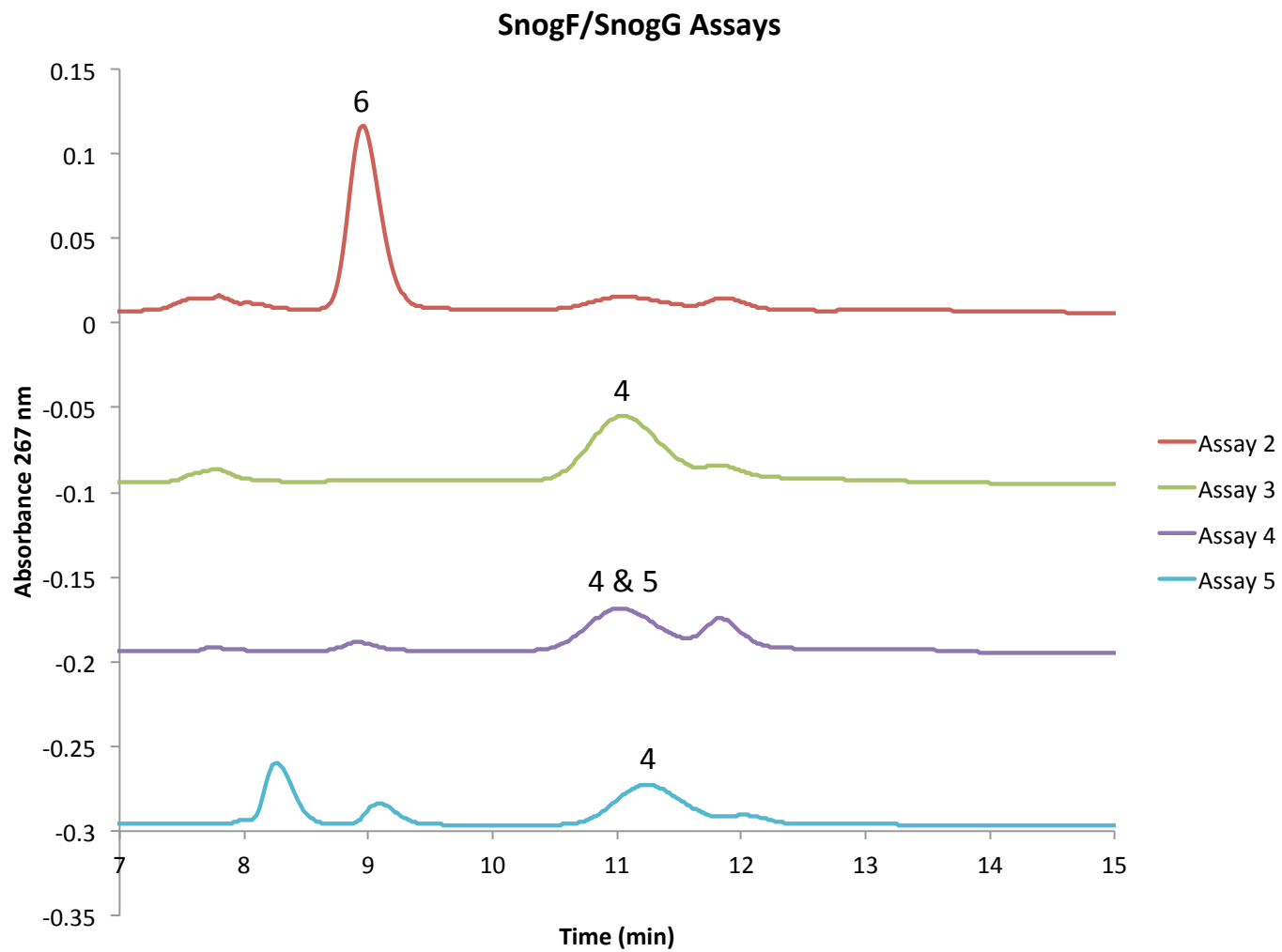
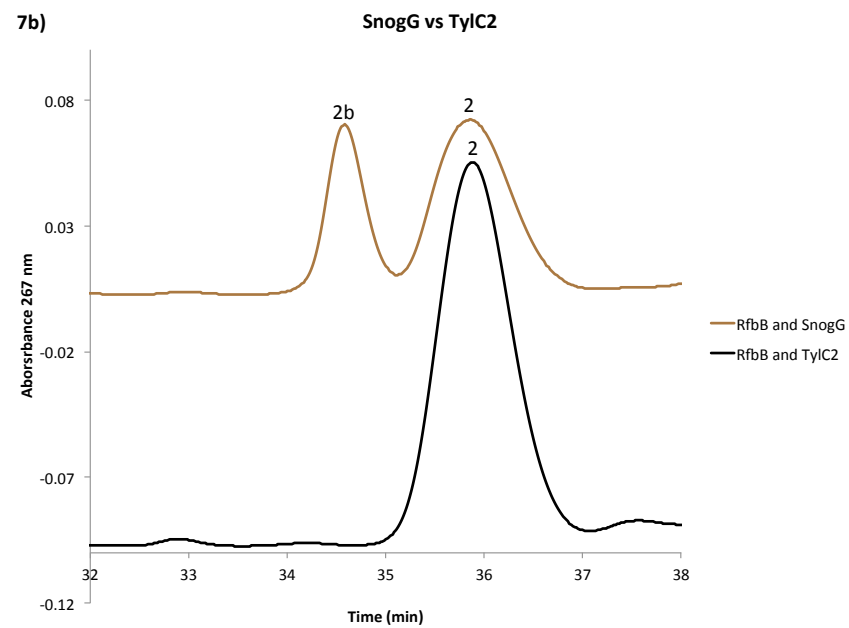
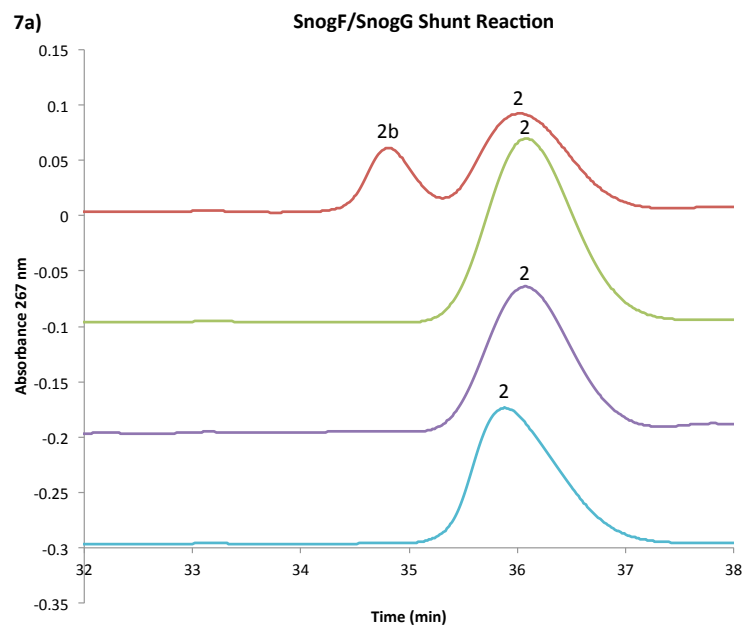


Figure 6: HPLC traces for assays 2-5, looking at the role of SnogF and SnogG in the synthesis of nogalamine.



**Figure 7: SnogF and SnogG shunt reaction assays. a) Peaks seen in original SnogF/SnogG assays. b) Traces of assays containing RfbB, SnogF, and SnogG; and RfbB, SnogF, and TylC2.**

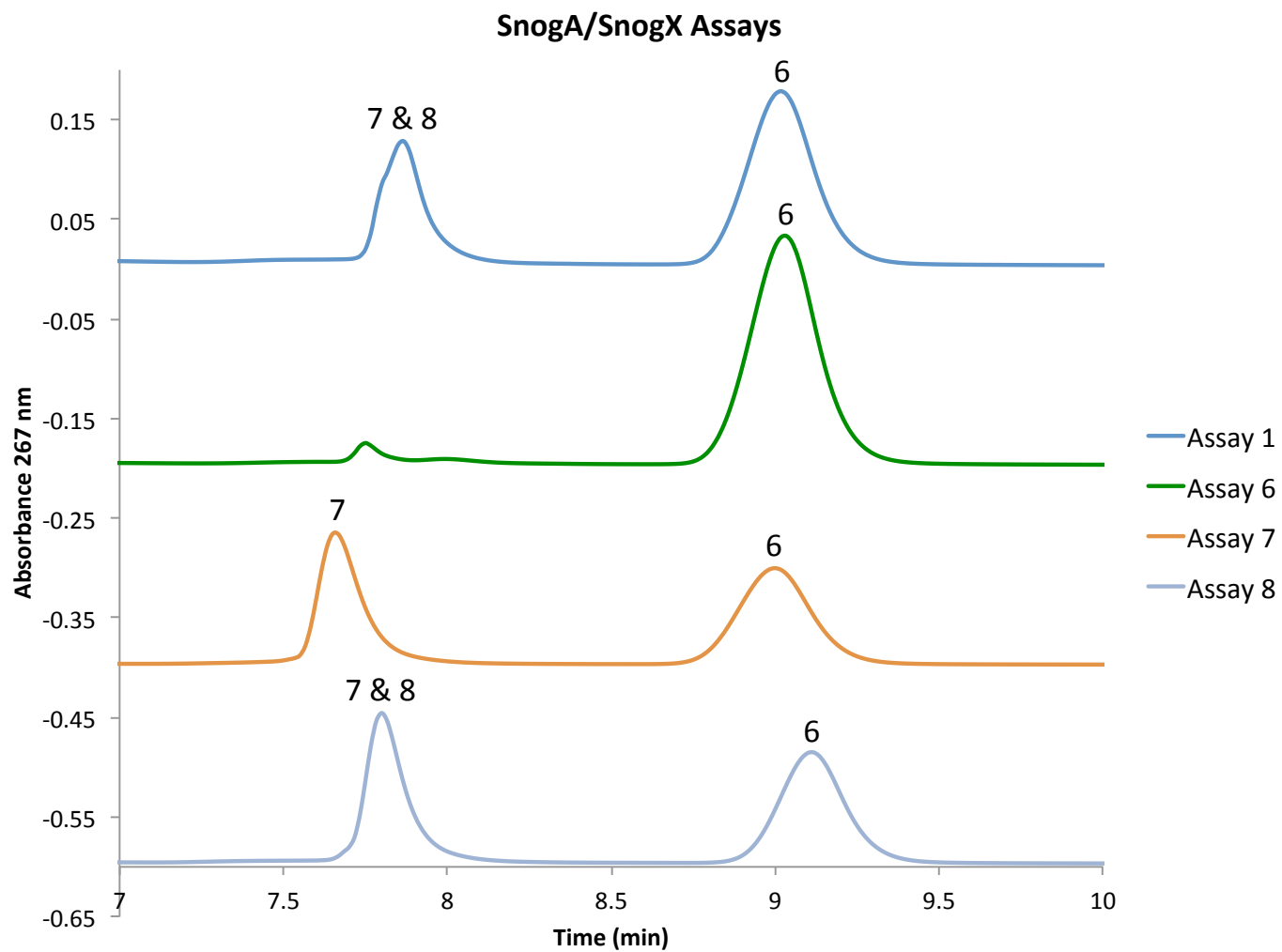


Figure 8: HPLC traces for assay 1 and assays 6-8. Trace for assay 1 is provided as a reference. Assays 6-7 investigate the role of SnogA and SnogX in the methylation of nogalamine.

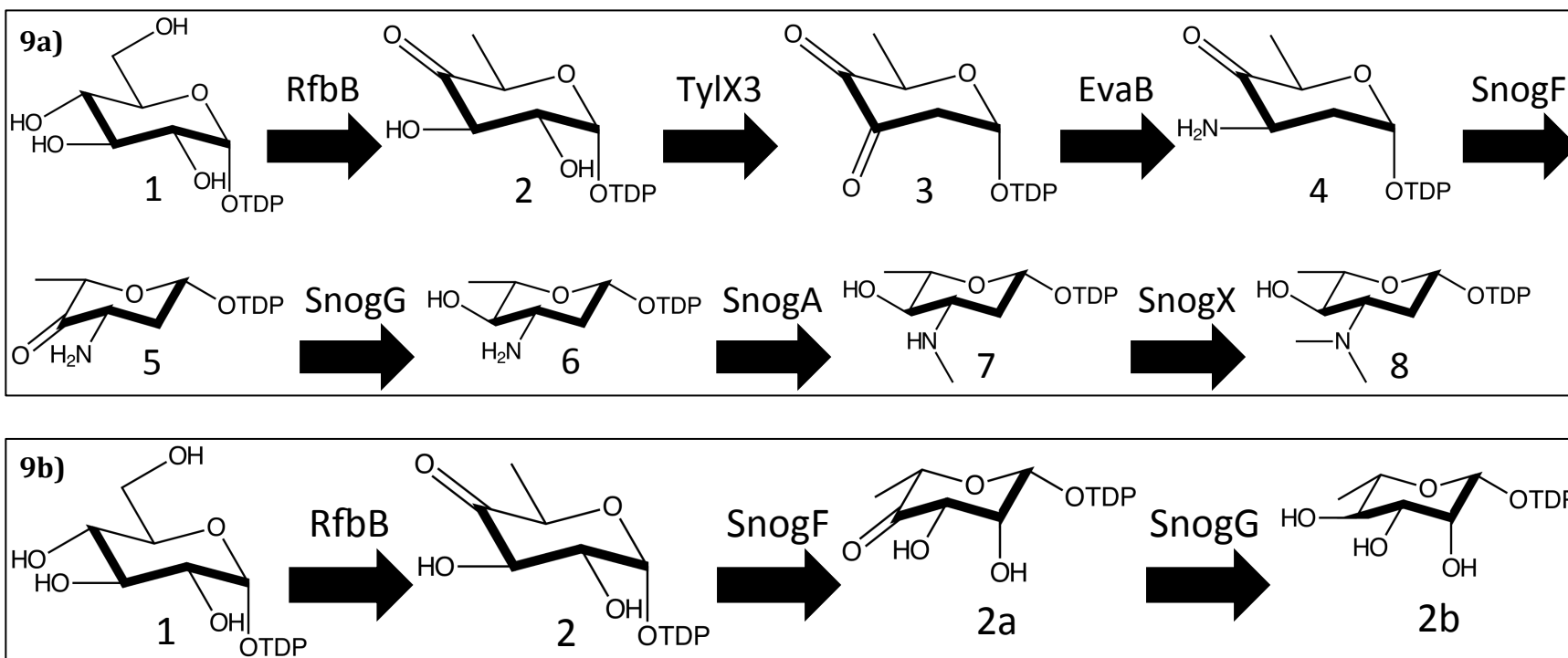


Figure 9: a) Biosynthesis pathway for TDP-2-deoxynogalamine. b) Shunt pathway for SnogF and SnogG to nogalose biosynthesis.